Tohoku J. Exp. Med., 2024, **263**, 199-210

Arsenic Trioxide Induces Retinoic Acid-Related Orphan Receptor Beta and Blocks the WNT Pathway to Inhibit Stemness in Glioblastoma

Dacheng Ding,[1] Kaiming Gao,[1] Xuebin Zhang[2] and Hu Wang[1,3]

[1]Department of Neurosurgery, Tianjin Huanhu Hospital, Tianjin, P.R. China
[2]Department of Pathology, Tianjin Huanhu Hospital, Tianjin, P.R. China
[3]Tianjin Key Laboratory of Cerebral Vascular and Neurodegenerative diseases, Tianjin Neurosurgical Institute, Tianjin, China

Glioblastoma (GBM) is a malignant primary brain tumor and an essential contributor to morbidity and mortality globally. Arsenic trioxide (ATO) exerts specific roles in preventing tumor growth. This study investigated the role of ATO in GBM cell behaviors and stemness. The effects of ATO on the malignant behavior of GBM cells, tumor stemness, and epithelial-mesenchymal transition (EMT) factors in mouse tumor tissues were explored. Targets of ATO in GBM were predicted using multiple databases. Subsequently, the expression of retinoic acid-related orphan receptor beta (RORB), WNT-1, *β*-Catenin, and c-Myc expression were examined in GBM cells before and after ATO treatment. ATO inhibited the malignant behavior of GBM cells *in vitro* and slowed down the GBM growth *in vivo* by inhibiting the stemness. The inhibitory effect of ATO on GBM was achieved by promoting RORB levels and strengthening the antagonism to *β*-Catenin to inhibit Wnt signaling, thus inhibiting tumor growth. Collectively, ATO induced RORB levels in GBM cells and strengthened the antagonistic effect on *β*-Catenin, thus inhibiting WNT signaling and tumor growth.

Keywords: arsenic trioxide; *β*-Catenin; cell stemness; glioblastoma; WNT signaling pathway
Tohoku J. Exp. Med., 2024 July, **263** (3), 199-210.
doi: 10.1620/tjem.2024.J033

Introduction

Glioblastoma (GBM) is considered to derive from either neuroglial progenitor or stem cells and is primarily featured by high molecular heterogeneity, which represents the most prevalent type among malignant primary brain tumors and an essential contributor to morbidity and mortality globally (Wen et al. 2020). The incidence of GBM is roughly 3-5 per 100,000 individuals annually, and the median age at diagnosis is reported to be 65 years (McKinnon et al. 2021). Despite recent advances in multiple treatment modalities including surgery, pharmacotherapy (chemotherapy and concomitant temozolomide being the typical option), and radiotherapy, the outcomes for GBM patients remain unsatisfactory, with a median overall survival of 14.6-20.5 months (Rong et al. 2022). Cancer stem cells (CSCs), also well-known as tumor-initiating cells, are neoplastic cells possessing pluripotent and self-renewing features, which have attained remarkable academic interests owing to their significant roles in tumor recurrence and resistance to radiotherapy as well as chemotherapy (Biserova et al. 2021). Therefore, efforts are warranted in the investigation of tumor stemness during GBM progression to develop more effective treatment approaches and improve the outcomes of patients.

As a therapeutic agent for acute promyelocytic leukemia, arsenic trioxide (ATO) is shown to exert a specific role in preventing the growth of GBM cells, which can be used as an additional therapeutic modality to the standard chemotherapy for GBM (Bureta et al. 2019). Bio-fabricated nanodrugs carrying ATO can gather in tumor foci through various natural pathways and respond to the microenvironment, thereby achieving tumor cell proliferation suppression and real-time navigating diagnosis (Wang et al. 2023).

Received February 18, 2024; revised and accepted May 16, 2024; J-STAGE Advance online publication May 24, 2024
Correspondence: Hu Wang, Department of Neurosurgery, Tianjin Huanhu Hospital, No.6, Jizhao Road, Jinnan District, Tianjin 300350, P.R. China. Tianjin Key Laboratory of Cerebral Vascular and Neurodegenerative diseases, Tianjin Neurosurgical Institute, Tianjin, China.
e-mail: wangh3212@163.com

Our previous research has shown that ATO markedly reduced the clonogenic capacity of the tumor neurospheres, and the stem-like CD133-positive fraction was also diminished along with the expression of the stem cell markers SOX2 and CD133 (Ding et al. 2014). Consequently, investigating the molecular mechanisms of ATO in GBM stemness is of considerable importance.

Importantly, bioinformatics analysis revealed that retinoic acid-related orphan receptor beta (RORB) acted as a target of ATO and was downregulated in GBM. RORB plays vital roles in an array of biological and pathological processes, and the abnormal RORB-induced circadian rhythm has brought a novel direction for further investigations on tumorigenesis and cancer prevention strategies (Feng et al. 2015). In medulloblastoma (a pediatric central nervous system tumor), RORB is weakly expressed and associated with prognosis (Guo et al. 2021). RORB represses the tumorigenic ability and stemness of gastric cancer cells by reducing the WNT/β-Catenin pathway activity (Wen et al. 2021). Due to pleiotropic functions in stem cell proliferation and neurogenesis, the WNT/β-Catenin pathway is extensively implicated in GBM (Shahcheraghi et al. 2020). The WNT/β-Catenin pathway is upregulated in approximately 80% of GBM cases and leads to tumor initiation, development, and survival, indicating that targeting this cascade may become a therapeutic strategy for GBM (Precilla et al. 2022).

Considering the above research findings, we reasonably speculated that ATO may affect GBM stemness and progression through the regulation of RORB and the WNT/β-Catenin pathway. Herein, we arranged related experiments to validate our speculation, aiming at enlarging the knowledge of stemness and assisting in the management and therapy of GBM.

Materials and Methods

Cell culture

GBM cells T98G (Procell Life Science & Technology, Wuhan, Hubei, China) and U-87 (National Collection of Authenticated Cell Cultures, Shanghai, China) were cultured in a Dulbecco's modified Eagle's medium (DMEM) (21063029, Thermo Fisher Scientific Inc., Waltham, MA, USA) supplemented with 10% FBS (Thermo Fisher) and 1% penicillin-streptomycin (Thermo Fisher) in a humidified environment at 37°C with 5% CO_2. Every 10^5 GBM cells were treated with 2.5 μM ATO (A1010, Sigma-Aldrich Chemical Company, St. Louis, MO, USA) for 72 h (Ding et al. 2014). GBM cells were treated with 25 μM diluted ICG001 (WNT/β-Catenin inhibitor, SF6827-5mg, Beyotime Biotechnology Co., Ltd., Shanghai, China) according to the manufacturer's requirements for 8 h.

RORB knockdown and overexpression

RORB overexpression was induced by lentiviral vectors from Gene-Chem (Shanghai, China). RORB silencing was induced by lentiviral vectors-mediated RNAi (Gene-Chem). After transfection, positive cells were screened with 10 μg/mL puromycin. The lentiviral transfection effect was verified by qPCR (Jiang et al. 2022).

Colony formation assay

GBM cells before and after ATO treatment were plated in 6-well plates at 500 cells/well. After two weeks of cultivation at 37°C and 5% CO_2, the cells were rinsed three times with phosphate buffer saline (PBS), fixed in 4% paraformaldehyde solution (Shanghai Sangon Biological Engineering Technology & Services Co., Ltd., Shanghai, China) dissolved in 0.1 M phosphate buffer for 15 min, and stained with crystal violet (A600331, Sangon) for 10 min. The staining solution was then washed with PBS to calculate the number of cell populations or colonies formed by cell proliferation *in vitro*. The 6-well plate was inverted, covered with a grid, and counted under an optical microscope.

Cell counting kit (CCK)-8

To investigate the cytotoxicity of ATO on GBM, CCK-8 (ab228554, Abcam, Cambridge, MA, USA) was used to perform the assay. GBM cells were seeded in 12-well plates at 10^5 cells per well and 12 h later treated with 2.5 μM ATO for 72 h, and then 10 μL of CCK-8 solution was added to each well. After incubation at 37°C for 2 h, optical density was measured at 450 nm, and cell viability was calculated.

Transwell assay

The cell suspension (200 μL) containing 10^4 GBM cells treated with 2.5 μM ATO was paved in Transwell chambers of 24-well plates coated with Matrigel (CLS354234, Sigma-Aldrich), and the lower chambers were supplemented with fresh medium containing FBS. Cells were transferred to the incubator at 37°C/5% CO_2 for 24 h. Cells in the lower chambers were fixed using 4% paraformaldehyde for 15 min and stained with 1% crystal violet for 15 min. The number of invasive cells in the lower chambers was observed and counted in the microscope.

Wound healing assay

GBM cells treated with 2.5 μM ATO were cultured on culture plates. When grown to confluency in a monolayer, a line was drawn on the confluent monolayer using a pipette tip or a hard object to remove the cells by mechanical force. A blank area was artificially created, called a scratch. Cell debris was washed off, and photographs of the scratched areas were taken to measure the width. After 24 h of culturing with serum-free medium, the migration of cells to the scratched areas was observed, and the wound healing rate was calculated.

TUNEL

The TUNEL assay was analyzed according to the kit protocol (C1089, Beyotime). GBM cells were seeded on

chamber slides at 10^4 cells/mL for 24 h, treated with 2.5 μM ATO, fixed with 4% paraformaldehyde for 30 min, and permeabilized with 0.2% Triton X-100 (P0096, Beyotime) for 5 min (both at room temperature). The TUNEL assay solution was configured according to the instructions, followed by two washes with PBS at room temperature. Next, the cells were added with 50 μL of assay solution for 60 min at 37°C in the dark and sealed with an anti-fluorescence quenching agent. The cover glass was observed under the microscope.

Sphere formation assay

A total of 2,000 GBM cells treated with 2.5 μM ATO were seeded in 24-well ultralow cluster plates (Corning, NY, USA). The spheres were cultured in DMEM/F12 (11320033, Thermo Fisher) supplemented with EGF, FGF, B-27, and N-2. The formed spheres were observed under a microscope and photographed. After 14 d, the neurospheres were observed using a light microscope, and the diameter was measured.

Flow cytometry

GBM cells were cultured at 10^5 cells/well in DMEM with 10% FBS in 24-well plates for 6 h. GBM cells treated with 2.5 μM ATO were harvested and washed with cold PBS buffer, resuspended in binding buffer, and incubated with APC-CD133 (ab252129, Abcam) and PE-CD44 (ab269300, Abcam) for 30 min in the dark. After washing three times with PBS, cells were detected by flow cytometry and analyzed.

Western blot

GBM cells were lysed with RIPA buffer (89900, Thermo Fisher Scientific), and total protein was quantified using the BCA Protein Quantification Assay Kit (23229, Thermo Fisher Scientific). Equal amounts of total proteins were subjected to SDS-polyacrylamide gel by electrophoresis and then transferred to nitrocellulose membranes, which were incubated with Tris-buffered saline with Tween containing 4% skimmed milk for 1 h at room temperature. Membranes were then probed at 4°C overnight with primary antibodies anti-RORB (1:1,000, ab228650, Abcam), anti-CD133 (1:2,000, ab222782, Abcam), anti-SOX2 (1:1,000, ab92494, Abcam), anti-NANOG (1:1,000, ab109250, Abcam), anti-OCT4 (1:1,000, 2750S, CST, Beverly, MA, USA), anti-alpha Tubulin (1:7,000, ab176560, Abcam), anti-β-Catenin Antibody (1:1,000, 8480S, CST), anti-WNT1 (1:25, ab15251, Abcam), and anti-c-Myc (1:1,000, AF6513, Beyotime) and with horseradish peroxidase (HRP)-labeled goat anti-rabbit IgG (H+L) (1:1,000, A0208, Beyotime) at room temperature for 1 h. The chemiluminescence method was used to develop the protein bands, and ImageJ was utilized to analyze the grey value of the bands.

In vivo experiment

The Animal Care and Use Committee of Tianjin Huanhu Hospital approved all animal experiments. Immunodeficient 6-8-week-old BALB/c nude mice (Vital River, Beijing, China) were subcutaneously injected with U-87 cell suspension (100,000 cells/mL, total injection volume 0.2 mL/mouse) before and after ATO treatment and knockdown RORB combined with ATO treatment on the back, 6 mice in each group. Tumor volume was measured every 3 d. At the end of d 21, the nude mice were euthanized by intraperitoneal injection of an overdose of pentobarbital sodium (150 mg/kg), and the tumors were removed and weighed.

Immunohistochemistry

Immunohistochemistry was performed on paraffin-embedded sections fixed in 4% paraformaldehyde. Following routine deparaffinization and hydration, the sections were immersed in sodium citrate (0.01 M, pH = 6.0) for antigen retrieval overnight at 60°C. After covering the sections with 3% hydrogen peroxide for 10 min, they were blocked with 5% goat serum for 2 h at room temperature. Anti-Ki67 (1:1,000, ab15580, Abcam), Anti-SLUG (1:250, ABE993, Sigma-Aldrich), Anti-TWIST1 (1:200, PA5-49688, Thermo Fisher Scientific), and Anti-N-Cadherin [EPR1791-4] (1:50, ab76011, Abcam) were then used as primary antibodies. Goat anti-rabbit HRP-conjugated secondary antibody (1:500, AP132P, Sigma-Aldrich) was then incubated for 60 min at 37°C before development with 3, 3-diaminobenzidine. Sections were counterstained with hematoxylin, dehydrated with ethanol, cleared with xylene, mounted with neutral gum, and finally observed for cell positivity (%).

RT-qPCR

Total RNA was extracted using the TRizol method (15596026, Thermo Fisher Scientific). The quantity and quality of isolated RNA were detected with Nanodrop. Complementary DNA (cDNA) was synthesized using PrimeScript RT Master Mix (RR036Q, Takara Bio, Kusatsu, Shiga, Japan). RT-qPCR assays were performed by PCR LightCycler480 (Roche Diagnostics, Basel, Switzerland) using PowerTrack SYBR Green Master Mix (A46012,

Table 1. Primer sequences used in RT-qPCR.

Gene	Forward sequence (5′-3′)	Reverse sequence (5′-3′)
RORB	TGTGCCATCCAGATCACTCACG	GGTTGAAGGCACGGCACATTCT
β-actin	CACCATTGGCAATGAGCGGTTC	AGGTCTTTGCGGATGTCCACGT

Note: RT-qPCR, reverse transcription quantitative polymerase chain reaction; RORB, retinoic acid-related orphan receptor beta.

Thermo Fisher Scientific). β-actin was used as endogenous control. Table 1 lists the primers used.

TOP-FOP flash luciferase reporter system

Firstly, 8 μL Fugene 6 (PRE2693, Roche Diagnostics) was incubated with 100 μL OPTI-MEM (51985091, Thermo Fisher Scientific) for 5 min at room temperature. Then, a total of 2 μg plasmid mixture consisting of TOP (21-170, Sigma-Aldrich), FOP (21-169, Sigma-Aldrich), and PRL (E2231, Promega, Madison, WI, USA) (4:4:1) was added to the above mixture and incubated for 15 min at room temperature. A mixture of Fugene 6 and plasmids was then added to a 6-well plate for a-24 h incubation at 37°C in a 5% CO_2 incubator. Luciferase activity was detected using the Dual-Luciferase Reporter Assay System (Promega).

Statistical analysis

All data analysis in the study was performed using GraphPad Prism 8.0.2 software (GraphPad, USA). An unpaired t-test was used to analyze differences between two groups, and one-way ANOVA and two-way ANOVA were used to compare multiple groups, with Tukey's test for post hoc test. $p < 0.05$ was considered statistically significant, and all data were presented as mean ± standard deviation (SD) from more than three independent experiments.

Results

ATO represses the malignant behavior of GBM cells

U-87 and T98G were treated with 0 μM, 1 μM, 2.5 μM, and 5 μM ATO for 72 h. Colony formation assay revealed that the number of colony-forming cells decreased with the increase in the dosage of ATO (Fig. 1A). GBM cells treated with 2.5 μM ATO for 72 h were utilized for subsequent assays. CCK-8 assay showed that after ATO treatment, the viability of GBM cells was significantly decreased (Fig. 1B). Wound healing assay presented that the healing ability of GBM cells was greatly diminished after ATO treatment (Fig. 1C). TUNEL assay determined that the percentage of GBM cell apoptosis was notably increased after ATO treatment (Fig. 1D). Transwell assay verified that the migration and invasion of GBM cells were markedly reduced after ATO treatment (Fig. 1E).

ATO suppresses the stemness of GBM stem cells

To investigate the effect of ATO on GBM cell stemness, T98G and U-87 were used to test the sphere-forming ability. The sphere-forming ability of GBM treated with ATO at 2.5 μM was significantly decreased (Fig. 2A). Western blot analysis indicated that the levels of stemness markers (CD133, SOX2, NANOG, and OCT4) were downregulated in ATO-treated GBM cells, whereas higher in untreated GBM cells (Fig. 2B). Subsequently, U-87 cells before and after ATO treatment were inoculated into nude mice to assess the effects of ATO on the tumorigenic ability and stemness of GBM cells *in vivo*, and the changes in tumor volume before and after ATO treatment were observed. After 21 d, the mice were euthanized, and the tumors were weighed (Fig. 2C). The levels of stemness markers in tumors were reduced after ATO treatment (Fig. 2D). EMT is associated with stemness in CSC cells (Srivastava et al. 2018), so the expression of EMT factors (SLUG, TWIST1, and N-Cadherin) was detected by immunohistochemistry. ATO significantly downregulated the expression of SLUG, TWIST1, and N-Cadherin in tumors (Fig. 2E). These results suggest that ATO may disrupt cell stemness in GBM.

ATO increases RORB levels in GBM cells

Transcriptome profiling of fresh paired normal and tumor tissue samples in GBM patients (n = 12) from the GSE151352 dataset were analyzed setting adj. *p*. value (corrected by Benjamini & Hochberg) < 0.05, and a total of 3,353 differentially expressed genes (DEGs) were screened out (Fig. 3A). Then, we predicted the targets of ATO in the Super-PRED database (https://prediction.charite.de/index.php) and cross-screened the DEGs with |LogFC| > 2 with the targets predicted by the Super-PRED database. The results showed a total of four intersecting genes: KIT, RORB, NLK, and NR3C2 (Fig. 3B). Their protein expression in GBM was further analyzed in the Proteomics analysis of the UALCAN database (https://ualcan.path.uab.edu/index.html) (Fig. 3C). NLK was not included, while NR3C2 was not differentially expressed. The expression of RORB and KIT was significantly reduced in GBM. The probability of both as ATO targets was analyzed in Super-PRED database prediction results, and the probability of RORB (0.5205 *vs.* 0.5039) was higher.

Western blot results showed increased RORB expression after ATO treatment (Fig. 3D). The expression of RORB in GBM cells was downregulated, and RT-qPCR and western blot analysis verified the knockdown efficiency (Fig. 3E). The cells after infection were subjected to ATO (2.5 μM) treatment. Colony formation assay showed more colonies formed by GBM cells after *RORB* knockdown (Fig. 3F). CCK-8 assay showed that the viability of GBM cells was enhanced after *RORB* knockdown (Fig. 3G). The wound healing assay manifested the healing ability of GBM cells was greatly enhanced after *RORB* knockdown (Fig. 3H). TUNEL assay revealed that the apoptosis rate of GBM cells after *RORB* knockdown was significantly reduced (Fig. 3I). Transwell assay detected that the migration and invasion of GBM cells after *RORB* knockdown was significantly enhanced (Fig. 3J). The spherical tumor-forming ability of GBM cells was enhanced after RORB knockdown (Fig. 3K). After the knockdown of *RORB*, the protein expression of CSC markers (CD133, SOX2, NANOG, and OCT4) in GBM cells was significantly increased (Fig. 3L). Flow cytometry results showed that the proportion of $CD133^+CD44^+$ cells was increased after *RORB* knockdown (Fig. 3M).

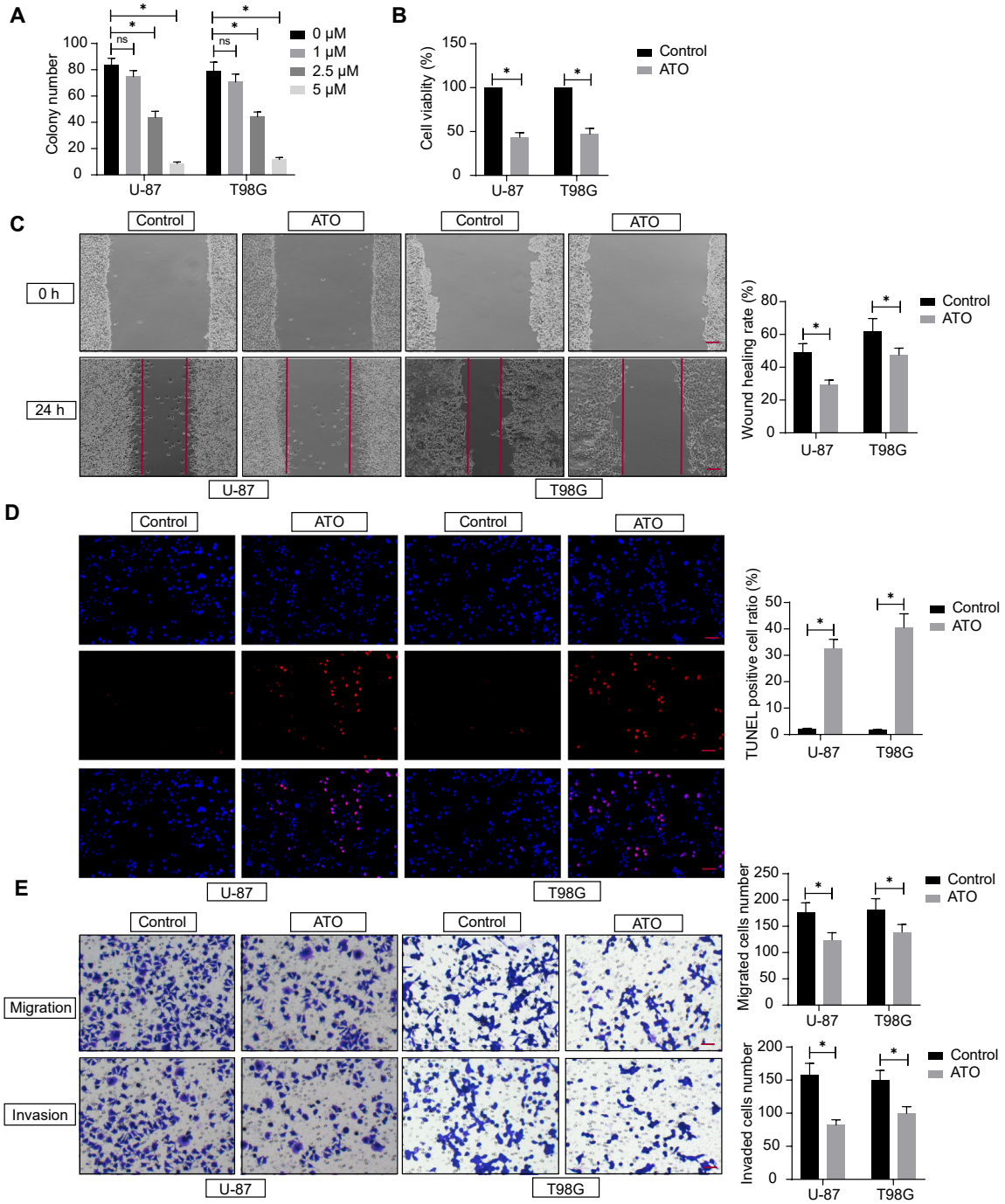

Fig. 1. ATO suppresses the malignant behavior of GBM cells.
A, Colony formation assay to investigate the colony formation ability of GBM cells; B, CCK-8 assay to detect GBM cell viability treated with 2.5 μM ATO; C, Wound healing assay to determine the healing of GBM cells treated with 2.5 μM ATO, Scale bar: 100 μm; D, TUNEL assay to determine the apoptosis ratio of GBM cells treated with 2.5 μM ATO, Scale bar: 25 μm; E, Transwell assay to verify migration and invasion ability of GBM cells treated with 2.5 μM ATO, Scale bar: 50 μm. The experiments were repeated three times independently, and two-way ANOVA analyzed comparisons among multiple groups, $*p < 0.05$.

RORB impairs the WNT signaling pathway

In gastric cancer, RORB was reported to inhibit gastric cancer cell stemness by blocking the WNT pathway (Wen et al. 2021). More relevantly, the WNT/β-Catenin cascade in GBM is a potential target to regulate CSC activity (Shevchenko et al. 2020), and the WNT pathway deficit is associated with GBM stemness inhibition (Wang et al. 2022). Therefore, we hypothesized that the effects of ATO on the malignant behavior of GBM and cancer stemness were related to the inhibition of WNT pathway transduction mediated by RORB restoration. After ATO treatment, the TOP/FOP luciferase activity was reduced (Fig. 4A). We

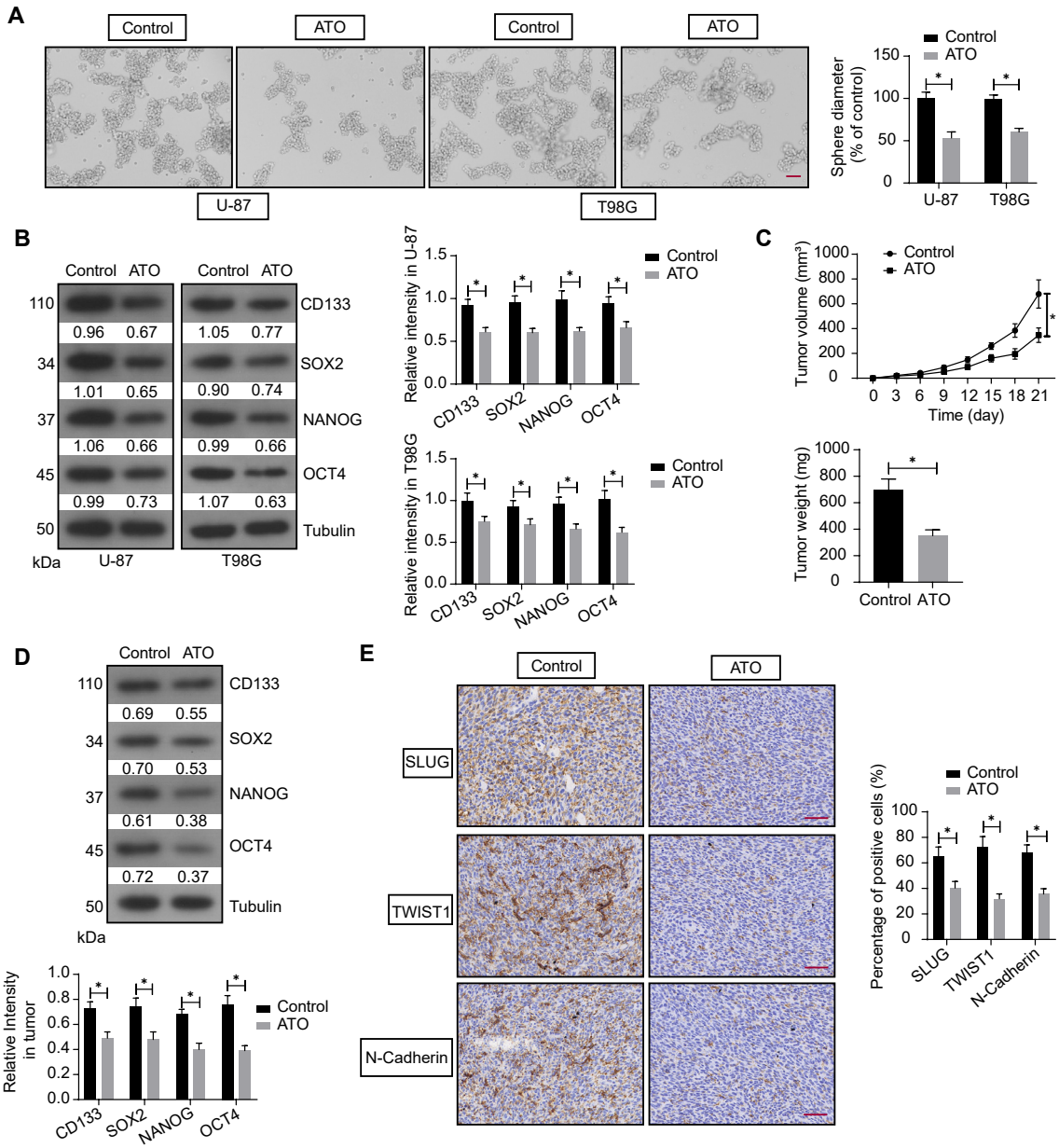

Fig. 2. ATO represses cell stemness in GBM.

A, Sphere capacity test was performed, Scale bar: 50 μm; B, Western blot detected the expression of glioma stem cell (GSC) stemness markers (CD133, SOX2, NANOG, and OCT4); C, Xenograft tumors were established to analyze the effect of ATO on tumor formation; D, Western blot detected the levels of stemness markers (CD133, SOX2, NANOG, and OCT4) in the xenograft tumors; E, Immunohistochemistry detected levels of EMT factors in the xenograft tumors, Scale bar: 50 μm. Unpaired t-test analyzed the comparisons between two groups, and two-way ANOVA analyzed the comparisons among multiple groups (n = 6), * $p < 0.05$.

treated GBM cells with ATO after *RORB* knockdown (KD-*RORB*) and overexpression (OE-*RORB*), and RT-qPCR verified the successful overexpression (Fig. 4B). WB assay showed that the KD-*RORB* group had elevated protein expression of WNT-1, β-Catenin, and c-Myc, and OE-*RORB* group had reduced expression of these proteins (Fig. 4C). TOP/FOP luciferase activity was elevated in GBM cells in the KD-*RORB* group, and in the OE-*RORB* group, TOP/FOP luciferase activity was decreased (Fig. 4D). The above experiments confirmed that *RORB* knockdown slows down the inhibition of ATO on β-Catenin and enhances the WNT pathway, thus promoting GBM progression.

ATO induces RORB expression and inhibits WNT signaling-mediated stemness in GBM cells

The Wnt inhibitor ICG001 was applied based on GBM cells treated with ATO after knocking down RORB. Western blot assay detected a decrease in the content of β-catenin in the GBM cells after treatment with ICG001 (Fig. 5A). Wnt inhibitor treatment significantly reduced TOP/FOP luciferase activity in GBM cells (Fig. 5B). The

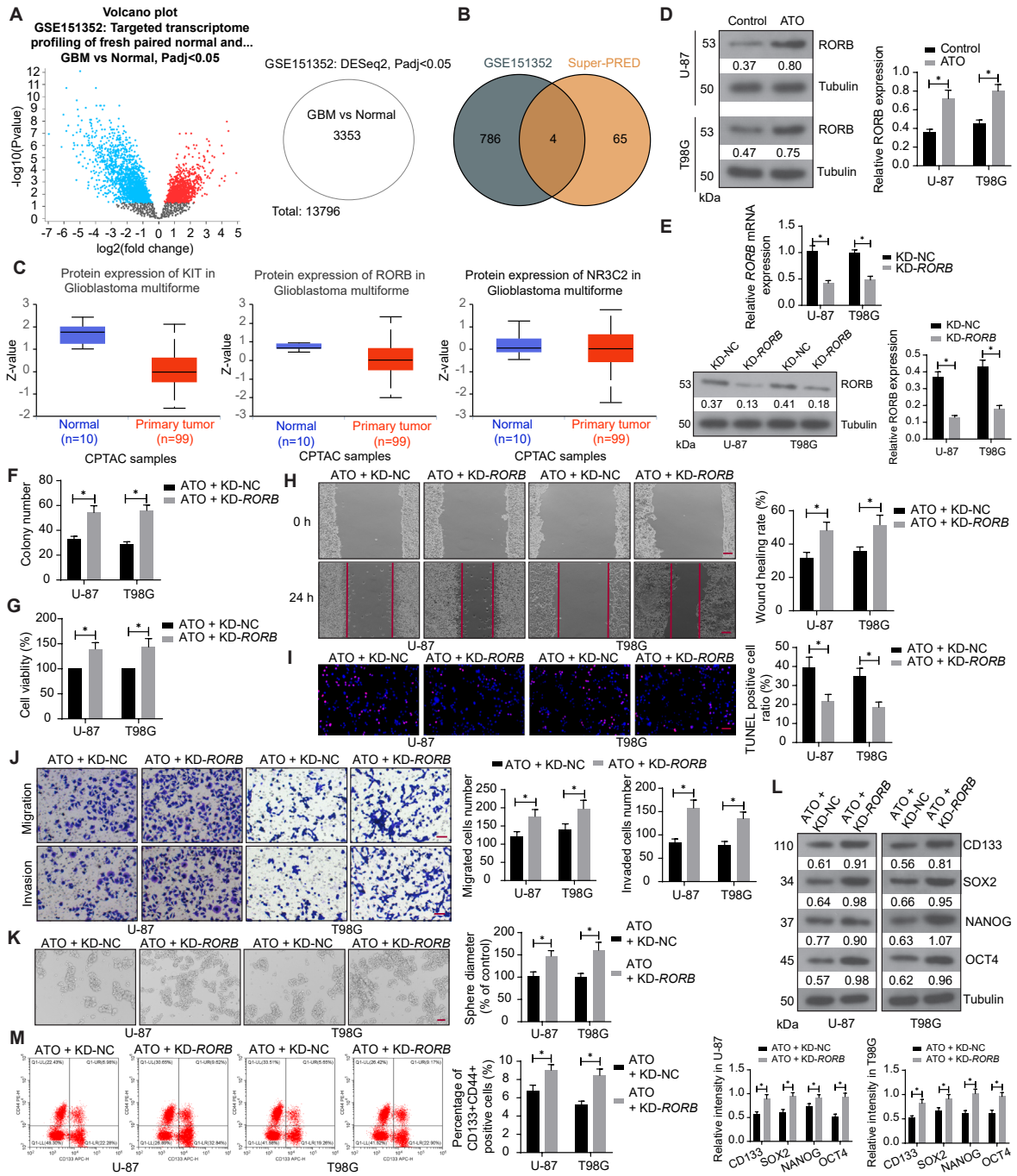

Fig. 3. The therapeutic effect of ATO on GBM is associated with enhanced RORB expression.

A, Differentially expressed genes in normal tissues and tumor tissues in the GSE151352 dataset; B, differentially expressed genes with |LogFC| > 2 were cross-screened with targets of ATO predicted by Super-PRED database; C, The expression of KIT, RORB, and NR3C2 in GBM in the UALCAN database; D, Western blot assay to detect the level of RORB in GBM cells treated with or without ATO; E, Lentiviral transfection to knock down RORB and RT-qPCR and western blot to verify the knockdown efficiency; F, Colony formation assay to investigate the colony forming ability of GBM cells after infection and 2.5 μM ATO treatment; G, CCK-8 assay to determine the viability of GBM cells after infection and 2.5 μM ATO treatment; H, Wound healing assay to determine the healing capacity of GBM cells after infection and 2.5 μM ATO treatment, Scale bar: 100 μm; I, TUNEL assay to determine the apoptosis rate of GBM cells after infection and 2.5 μM ATO treatment, Scale bar: 25 μm; J, Transwell assay to detect the migratory and invasive abilities of GBM cells after infection and 2.5 μM ATO treatment, Scale bar: 50 μm; K, Detection of sphere tumor-forming ability of GBM cells after infection and 2.5 μM ATO treatment, Scale bar: 50 μm; L, Western blot detection of CSC markers (CD133, SOX2, NANOG, and OCT4) in GBM cells after infection and 2.5 μM ATO treatment; M, Flow cytometry detection of the proportion of $CD133^{+}CD44^{+}$ cells in GBM cells after infection and 2.5 μM ATO treatment. The experiments were repeated three times independently, and two-way ANOVA analyzed comparisons among multiple groups, * $p < 0.05$.

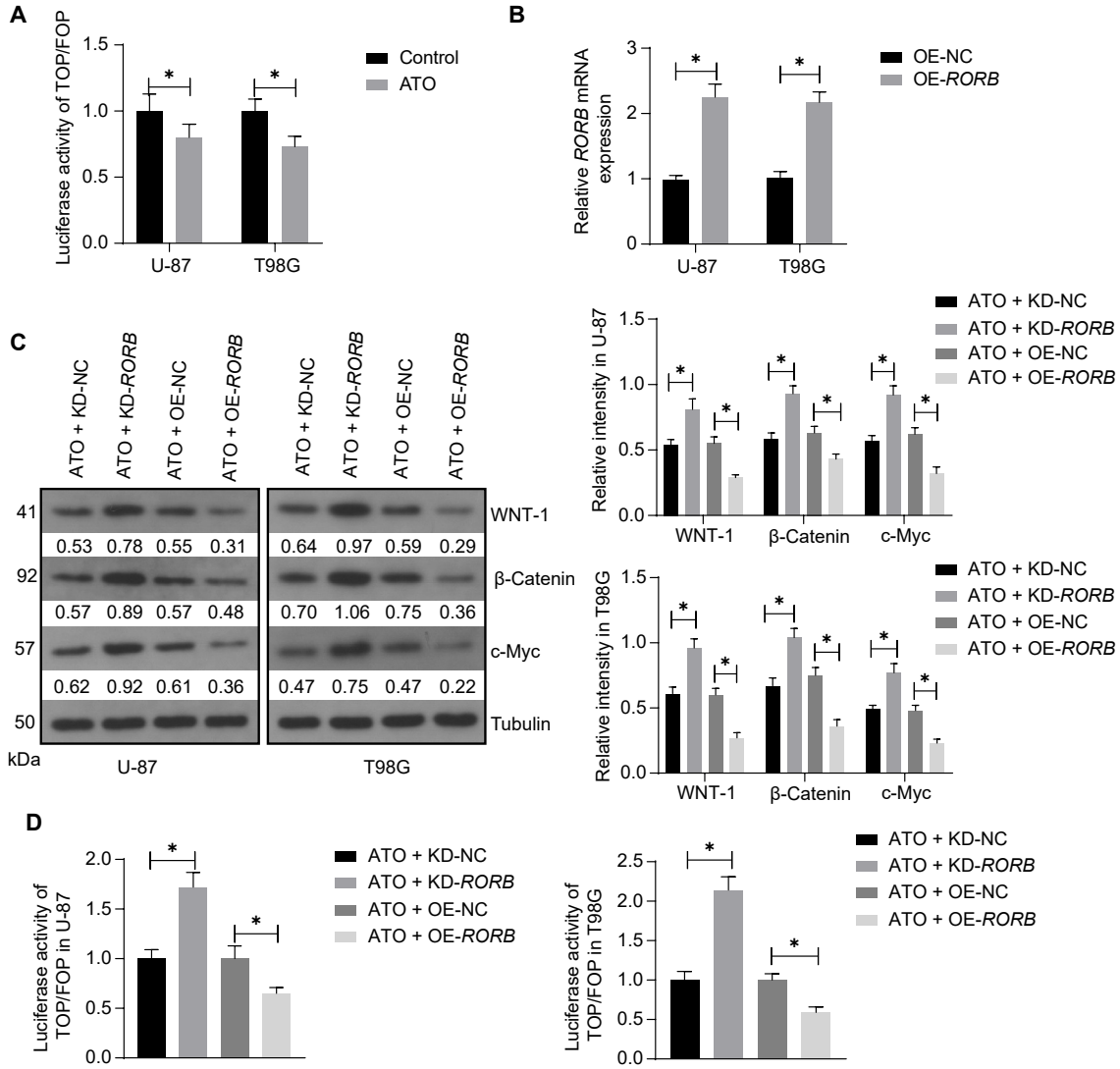

Fig. 4. RORB inhibits WNT signaling transduction.
A, TOP-FOP Flash luciferase reporter system was used to detect WNT signaling in GBM cells; B, RT-qPCR to verify the efficiency of RORB overexpression; C, Western blot to detect WNT-1, *β*-Catenin, and c-Myc expression in GBM cells; D, TOP/FOP luciferase activity was detected in GBM cells; the experiments were repeated three times independently, and one-way or two-way ANOVA analyzed the comparisons among multiple groups, $*p < 0.05$.

spherical tumor-forming ability was weakened by Wnt inhibitor treatment (Fig. 5C). The expression of CD133, SOX2, NANOG, and OCT4, CSC markers, (Fig. 5D) and the proportion of CD133-positive cells (Fig. 5E) were significantly reduced by Wnt inhibitor treatment.

ATO restricts the growth of GBM cells in vivo

Subcutaneous injection of U-87 cell suspension with knockdown of RORB after ATO treatment on the back of nude mice was performed to establish xenograft tumors, and observations were made every three d. The nude mice were euthanized on d 21, and tumors were removed and weighed. Xenograft tumors generated from GBM cells with the knockdown of RORB grew faster and yielded larger tumors (Fig. 6A). Immunohistochemistry revealed that the proportion of Ki67-positive cells in tumor tissues established by GBM cells knocked down by RORB was elevated (Fig. 6B). Stemness markers CD133, SOX2, NANOG, and OCT4 significantly elevated after *RORB* knockdown. WNT-1, *β*-Catenin, and c-Myc levels significantly elevated after the knockdown of RORB (Fig. 6C). Immunohistochemistry elicited increased levels of EMT factors (SLUG, TWIST1, N-Cadherin) in the tumor after *RORB* knockdown (Fig. 6D).

Discussion

GBM occurrence, progression, recurrence, and resistance to diverse therapies are intrinsically related to glioma stem cells (GSCs), as GSCs show self-renewal capacity, high proliferative rate, and the potential to differentiate into all sorts of distinct cell types, contributing to tumor heterogeneity (Stevanovic et al. 2021). As an FDA-approved

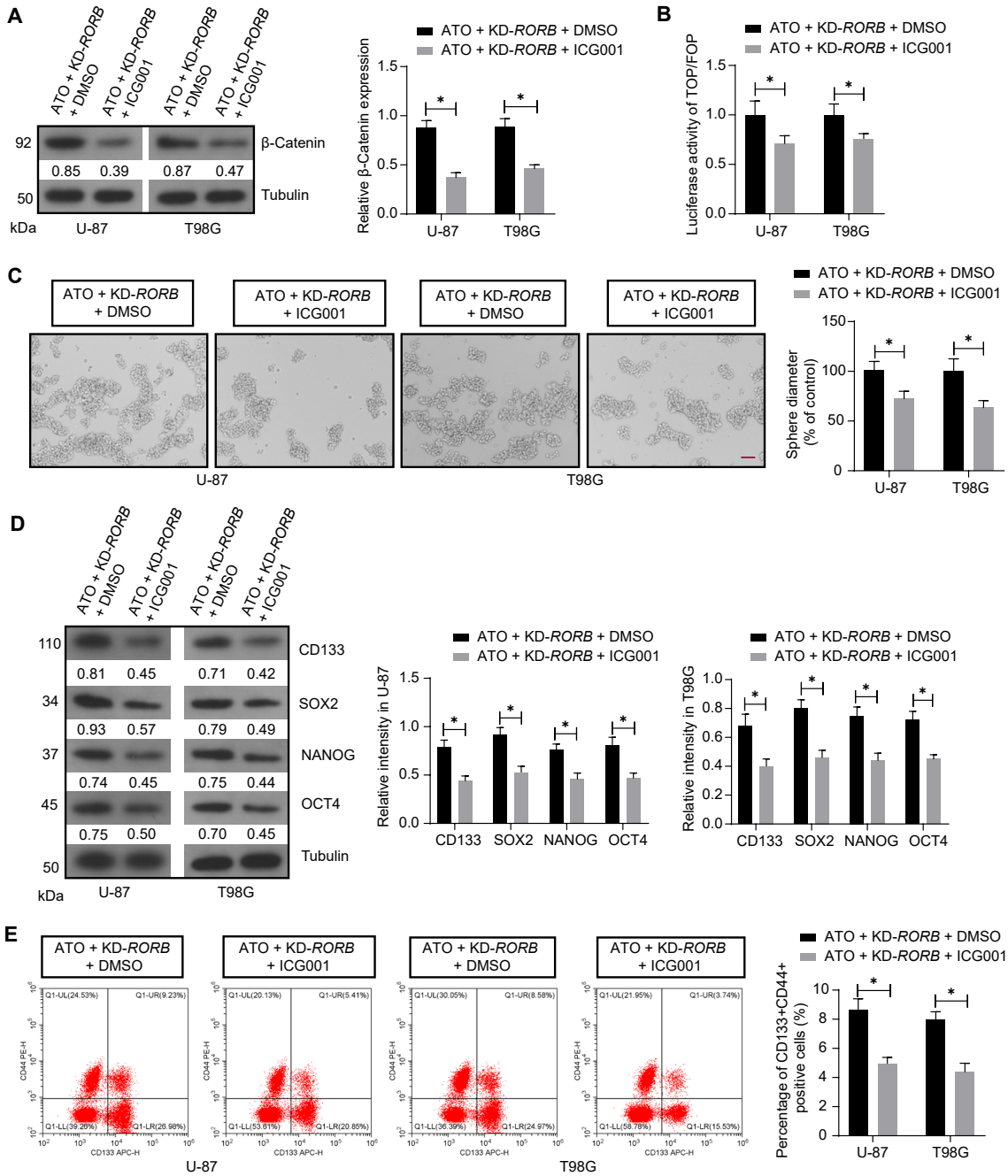

Fig. 5. WNT signaling inhibitor rescues the effects of RORB knockdown on GBM cells.
A, Western blot detection of *β*-Catenin expression in GBM cells; B, TOP-FOP flash luciferase reporter system to detect WNT signaling in GBM cells; C, Detection of sphere tumor formation ability, Scale bar: 50 μm; D, Western blot detection of CSC markers CD133, SOX2, NANOG, and OCT4 expression; E, Flow cytometry to detect the number of $CD133^{+}CD44^{+}$ cells. The experiments were repeated three times independently; two-way ANOVA analyzed comparisons among multiple groups, $*p < 0.05$.

drug capable of crossing the blood-brain barrier, ATO exhibits pre-clinical efficacy against GSCs in part via autophagy and apoptosis activation and Hedgehog pathway inhibition (Bell et al. 2018). Herein, this research explored the precise molecular mechanisms of ATO in mediating GBM progression, and the results evinced that ATO induced RORB expression and impeded the WNT/*β*-Catenin signaling to decrease tumor malignancy and stemness in GBM.

ATO is well-tolerated and safe when locally delivered into glioma, and it shows promise for local chemotherapy in the treatment of patients with newly diagnosed glioma (Han et al. 2022). The combination of temozolomide with nanodrugs carrying ATO effectively enhances the survival of GBM-bearing mice and lowers the recurrence rate (Wang et al. 2023). ATO combined with erlotinib considerably stimulates G2/M cell cycle arrest, decreases metabolic

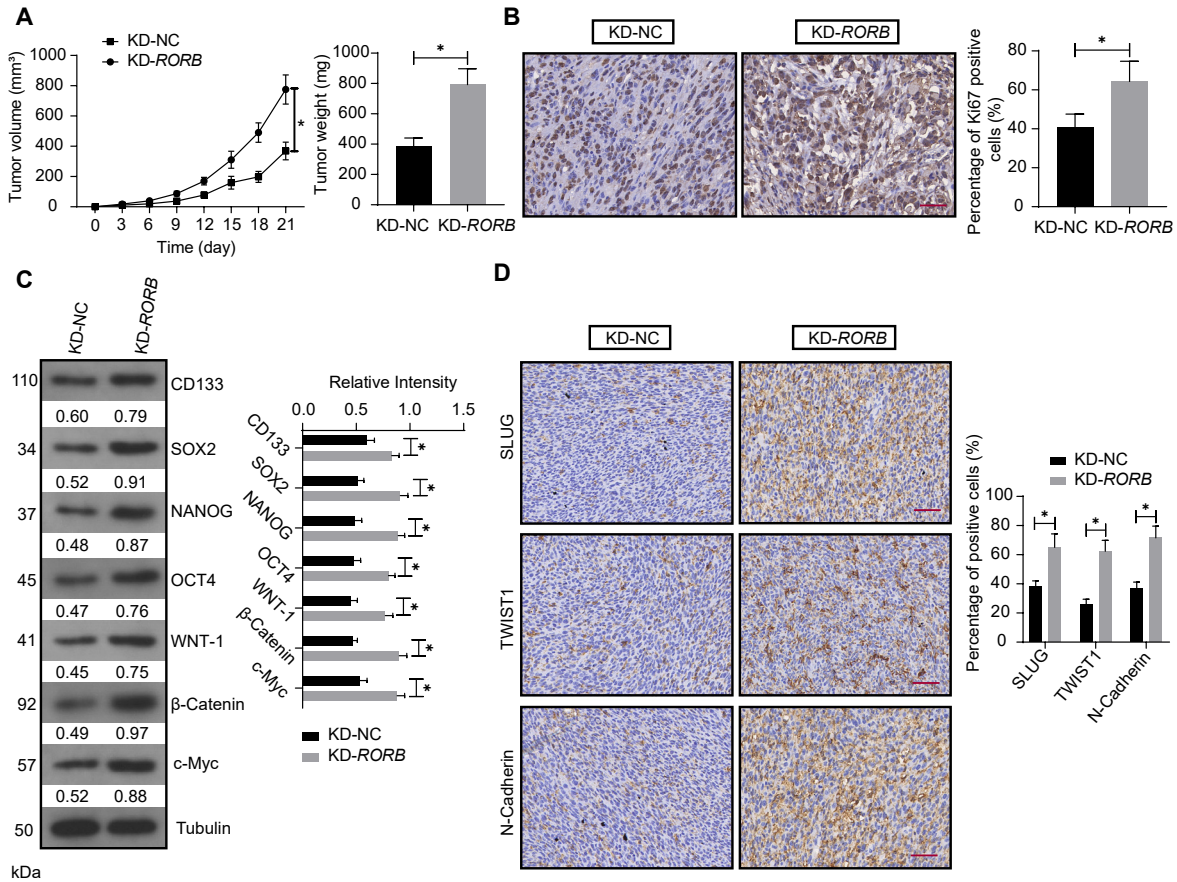

Fig. 6. ATO inhibits the Wnt pathway by promoting RORB expression and thus inhibits GBM *in vivo*.
A, U-87 cells were used to establish xenograft tumors to investigate the effect of RORB knockdown on tumor formation; B, The proportion of Ki67-positive cells in tumor tissues was determined by immunohistochemistry, Scale bar: 25 μm; C, Western blot to determine the expression of CD133, SOX2, NANOG, OCT4, WNT-1, β-Catenin, and c-Myc in tumors; D, Immunohistochemical assay to detect the levels of EMT factors (SLUG, TWIST1, N-Cadherin) in tumors, Scale bar: 50 μm. Unpaired t-test and two-way ANOVA were used for comparisons among multiple groups (n = 6), $^*p < 0.05$.

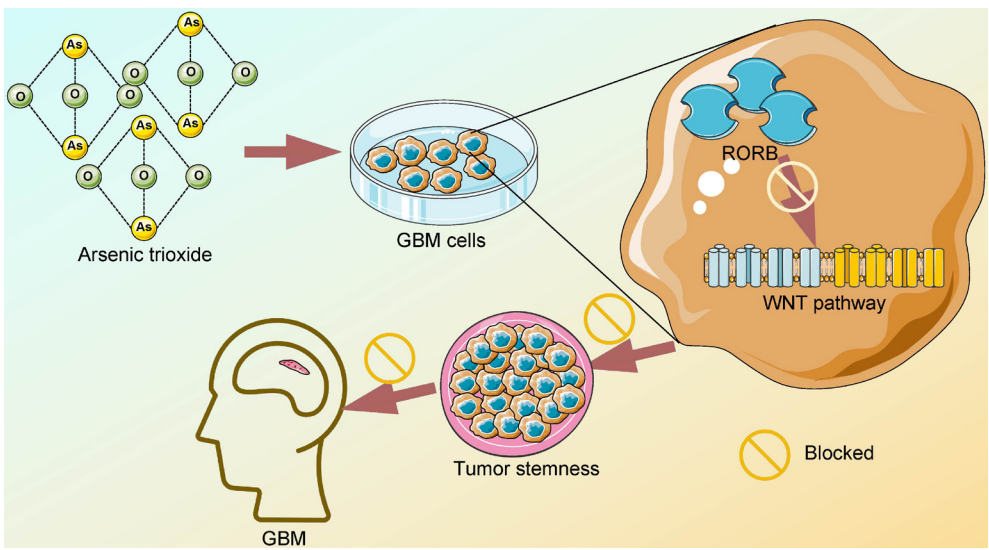

Fig. 7. Illustration of the regulatory mechanism.
Arsenic trioxide treatment activates RORB and thus blocks the WNT signaling pathway to impede GBM progression by repressing tumor stemness.

activity, colony-forming potential, proliferation, and migration, and enhances apoptotic death of GBM cells (Mesbahi et al. 2018). ATO is shown to stimulate apoptosis and autophagy in glioma cells and accelerate the differentiation of GSCs into non-tumorigenic cells (Carmignani et al. 2014). Expectedly, ATO repressed the malignant behaviors of GBM cells, manifested as a reduction in cell colony formation, viability, migration, and invasion, as well as enhancement in apoptosis. In terms of stemness, ATO weakened sphere formation capability and diminished expression levels of CSC markers, such as CD133, SOX2, NANOG, and OCT4. Sphere-forming capacity represents a well-known hallmark of GSCs *in vitro*, and ATO treatment can restrain sphere-forming and downregulate stemness markers OLIG2, SOX2, and SOX9 (Linder et al. 2019). ATO depletes CSCs in GBM and represses the repopulation of neurospheres by downregulating the Notch pathway (Wu et al. 2013). Here, ATO treatment curbed tumor development, stemness, and EMT *in vivo*. Interestingly, tumor cells undergoing EMT easily acquire stem-like features, indicating the close association between EMT and cancer stemness (Giordano et al. 2023). Accumulating reports have uncovered the suppressive impact of ATO on cancer EMT (Kim et al. 2018; Fan et al. 2019). Taken together, ATO conferred inhibitory functions in malignant behaviors and stemness of GBM.

Subsequently, the targets of ATO were screened. Results suggested the high probability of RORB as a target of ATO and its downregulation in GBM. Further experiments elicited that ATO elevated RORB expression in GBM cells. Silencing of *RORB* potentiated GBM cell growth and stemness and blocked apoptosis. A preceding study has uncovered that RORA impedes invasion, migration, and EMT of GBM by negatively mediating the TGF-β1/Smad pathway (Zhao et al. 2021). Several reports have unraveled the involvement of RORB in other cancers. For instance, RORB is lowly expressed in colorectal cancer and its overexpression reduces tumorigenic capacity, sphere-forming efficiency, and $CD44^{+}CD24^{+}$ CSCs (Wen et al. 2017). RORB weakens the stemness of gastric cancer cells via inactivation of the WNT/β-Catenin pathway, evidenced by decreased sphere-forming ability and downregulated CSC markers (Wen et al. 2021). Overall, these findings elucidated that ATO prevented GBM progression by upregulating RORB.

Compelling evidence suggests that GBM pathogenicity is partly attributed to the dysregulated WNT/β-Catenin signaling (Jamalpour et al. 2023). The WNT/β-Catenin pathway is considered a key mediator of biological functions including cell proliferation, metabolism, angiogenesis, and EMT, and targeting this pathway can disrupt critical functions of brain tumor cells to attain critical progress in alternative GBM therapeutic strategies, thus enhancing the survival of GBM patients (Barzegar Behrooz et al. 2022). Of note, ATO is revealed to potentiate tumor cell apoptosis and suppress viability in part via downregulation of the WNT/β-Catenin pathway in mantle cell lymphoma (Li et al. 2017) and prostate cancer (Zheng et al. 2016). In this study, the activity of the WNT/β-Catenin pathway in GBM cells was decreased by ATO treatment. Additionally, *RORB* knockdown activated the WNT/β-Catenin pathway, whereas RORB overexpression unleashed the contrary role. Previous research has unearthed that the WNT pathway activity is strongly weakened by RORB overexpression in colorectal cancer, indicating the role of RORB as an inhibitor of the WNT pathway (Wen et al. 2017). It is noteworthy that molecular pathways are active contributors to the GBM stemness of GSCs, including WNT/β-Catenin (Ryskalin et al. 2019). Repression of the WNT/β-Catenin cascade confers vital roles in hindering EMT, invasion, migration, and stemness of GBM cells (Liu et al. 2019; Li et al. 2021). Consistently, our results unveiled that suppression of this pathway was capable of reducing GBM cell stemness. Furthermore, the promotion effects of *RORB* silencing on the WNT/β-Catenin pathway as well as tumor deterioration and stemness were observed in GBM mice.

In summary, the research findings highlighted that ATO treatment increased RORB expression to impair the WNT/β-Catenin pathway, thereby lowering tumor malignancy and stemness in GBM (Fig. 7). This paper may provide insight into new options for inhibiting tumor stemness and offer promising targets and therapeutic strategies for GBM management in the clinic. However, clinical data were lacking in this study. In the future, clinical trials will need to be conducted to support the obtained results. Exploring other action targets of ATO is also a new direction.

Acknowledgments

This research was supported by the Tianjin Education Commission Research Program Project (No. 22KJ280).

Conflict of Interest

The authors declare no conflict of interest.

References

Barzegar Behrooz, A., Talaie, Z., Jusheghani, F., Los, M.J., Klonisch, T. & Ghavami, S. (2022) Wnt and PI3K/Akt/mTOR Survival Pathways as Therapeutic Targets in Glioblastoma. *Int. J. Mol. Sci.*, **23**, 1353.

Bell, J.B., Eckerdt, F., Dhruv, H.D., Finlay, D., Peng, S., Kim, S., Kroczynska, B., Beauchamp, E.M., Alley, K., Clymer, J., Goldman, S., Cheng, S.Y., James, C.D., Nakano, I., Horbinski, C., et al. (2018) Differential Response of Glioma Stem Cells to Arsenic Trioxide Therapy Is Regulated by MNK1 and mRNA Translation. *Mol. Cancer Res.*, **16**, 32-46.

Biserova, K., Jakovlevs, A., Uljanovs, R. & Strumfa, I. (2021) Cancer Stem Cells: Significance in Origin, Pathogenesis and Treatment of Glioblastoma. *Cells*, **10,** 621.

Bureta, C., Saitoh, Y., Tokumoto, H., Sasaki, H., Maeda, S., Nagano, S., Komiya, S., Taniguchi, N. & Setoguchi, T. (2019) Synergistic effect of arsenic trioxide, vismodegib and temozolomide on glioblastoma. *Oncol. Rep.*, **41**, 3404-3412.

Carmignani, M., Volpe, A.R., Aldea, M., Soritau, O., Irimie, A., Florian, I.S., Tomuleasa, C., Baritchii, A., Petrushev, B., Crisan, G. & Valle, G. (2014) Glioblastoma stem cells: a new target for metformin and arsenic trioxide. *J. Biol. Regul. Homeost. Agents*, **28**, 1-15.

Ding, D., Lim, K.S. & Eberhart, C.G. (2014) Arsenic trioxide

inhibits Hedgehog, Notch and stem cell properties in glioblastoma neurospheres. *Acta Neuropathol. Commun.*, **2**, 31.

Fan, Z., He, J., Fu, T., Zhang, W., Yang, G., Qu, X., Liu, R., Lv, L. & Wang, J. (2019) Arsenic trioxide inhibits EMT in hepatocellular carcinoma by promoting lncRNA MEG3 via PKM2. *Biochem. Biophys. Res. Commun.*, **513**, 834-840.

Feng, S., Xu, S., Wen, Z. & Zhu, Y. (2015) Retinoic acid-related orphan receptor RORbeta, circadian rhythm abnormalities and tumorigenesis (Review). *Int. J. Mol. Med.*, **35**, 1493-1500.

Giordano, F., D'Amico, M., Montalto, F.I., Malivindi, R., Chimento, A., Conforti, F.L., Pezzi, V., Panno, M.L., Ando, S. & De Amicis, F. (2023) Cdk4 Regulates Glioblastoma Cell Invasion and Stemness and Is Target of a Notch Inhibitor Plus Resveratrol Combined Treatment. *Int. J. Mol. Sci.*, **24**, 10094.

Guo, Y., Li, S., Huang, P., Zhang, H. & Yu, C. (2021) Development of a prognostic model based on an immunogenomic landscape analysis of medulloblastoma. *Biosci. Rep.*, **41**, BSR20202907.

Han, D., Teng, L., Wang, X., Zhen, Y., Chen, X., Yang, M., Gao, M., Yang, G., Han, M., Wang, L., Xu, J., Li, Y., Shumadalova, A. & Zhao, S. (2022) Phase I/II trial of local interstitial chemotherapy with arsenic trioxide in patients with newly diagnosed glioma. *Front. Neurol.*, **13**, 1001829.

Jamalpour, S., Alinezhad, A., Sabah, J.T., Vazifehmand, R., Behrooz, A.B., Hamzah, A.S.A., Davazdahemami, A.A., Homaie, F.M. & Maddah, S.M. (2023) Modulating Wnt/beta-Catenin Signaling Pathway on U251 and T98G Glioblastoma Cell Lines Using a Combination of Paclitaxel and Temozolomide, A Molecular Docking Simulations and Gene Expression Study. *Chem. Pharm. Bull.* (*Tokyo*), **71**, 766-774.

Jiang, Y., Zhao, J., Li, R., Liu, Y., Zhou, L., Wang, C., Lv, C., Gao, L. & Cui, D. (2022) CircLRFN5 inhibits the progression of glioblastoma via PRRX2/GCH1 mediated ferroptosis. *J. Exp. Clin. Cancer Res.*, **41**, 307.

Kim, S.H., Yoo, H.S., Joo, M.K., Kim, T., Park, J.J., Lee, B.J., Chun, H.J., Lee, S.W. & Bak, Y.T. (2018) Arsenic trioxide attenuates STAT-3 activity and epithelial-mesenchymal transition through induction of SHP-1 in gastric cancer cells. *BMC Cancer*, **18**, 150.

Li, S.Z., Ren, K.X., Zhao, J., Wu, S., Li, J., Zang, J., Fei, Z. & Zhao, J.L. (2021) miR-139/PDE2A-Notch1 feedback circuit represses stemness of gliomas by inhibiting Wnt/beta-catenin signaling. *Int. J. Biol. Sci.*, **17**, 3508-3521.

Li, X.Y., Li, Y., Zhang, L., Liu, X., Feng, L. & Wang, X. (2017) The antitumor effects of arsenic trioxide in mantle cell lymphoma via targeting Wnt/beta-catenin pathway and DNA methyltransferase-1. *Oncol. Rep.*, **38**, 3114-3120.

Linder, B., Wehle, A., Hehlgans, S., Bonn, F., Dikic, I., Rodel, F., Seifert, V. & Kogel, D. (2019) Arsenic Trioxide and (-)-Gossypol Synergistically Target Glioma Stem-Like Cells via Inhibition of Hedgehog and Notch Signaling. *Cancers* (*Basel*), **11**, 350.

Liu, Q., Guan, Y., Li, Z., Wang, Y., Liu, Y., Cui, R. & Wang, Y. (2019) miR-504 suppresses mesenchymal phenotype of glioblastoma by directly targeting the FZD7-mediated Wnt-beta-catenin pathway. *J. Exp. Clin. Cancer Res.*, **38**, 358.

McKinnon, C., Nandhabalan, M., Murray, S.A. & Plaha, P. (2021) Glioblastoma: clinical presentation, diagnosis, and management. *BMJ*, **374**, n1560.

Mesbahi, Y., Zekri, A., Ahmadian, S., Alimoghaddam, K., Ghavamzadeh, A. & Ghaffari, S.H. (2018) Targeting of EGFR increase anti-cancer effects of arsenic trioxide: Promising treatment for glioblastoma multiform. *Eur. J. Pharmacol.*, **820**, 274-285.

Precilla, D.S., Kuduvalli, S.S., Purushothaman, M., Marimuthu, P., Muralidharan, A.R. & Anitha, T.S. (2022) Wnt/beta-catenin Antagonists: Exploring New Avenues to Trigger Old Drugs in Alleviating Glioblastoma Multiforme. *Curr. Mol. Pharmacol.*, **15**, 338-360.

Rong, L., Li, N. & Zhang, Z. (2022) Emerging therapies for glioblastoma: current state and future directions. *J. Exp. Clin. Cancer Res.*, **41**, 142.

Ryskalin, L., Gaglione, A., Limanaqi, F., Biagioni, F., Familiari, P., Frati, A., Esposito, V. & Fornai, F. (2019) The Autophagy Status of Cancer Stem Cells in Gliobastoma Multiforme: From Cancer Promotion to Therapeutic Strategies. *Int. J. Mol. Sci.*, **20**, 3824.

Shahcheraghi, S.H., Tchokonte-Nana, V., Lotfi, M., Lotfi, M., Ghorbani, A. & Sadeghnia, H.R. (2020) Wnt/beta-catenin and PI3K/Akt/mTOR Signaling Pathways in Glioblastoma: Two Main Targets for Drug Design: A Review. *Curr. Pharm. Des.*, **26**, 1729-1741.

Shevchenko, V., Arnotskaya, N., Zaitsev, S., Sharma, A., Sharma, H.S., Bryukhovetskiy, A., Pak, O., Khotimchenko, Y. & Bryukhovetskiy, I. (2020) Proteins of Wnt signaling pathway in cancer stem cells of human glioblastoma. *Int. Rev. Neurobiol.*, **151**, 185-200.

Srivastava, C., Irshad, K., Dikshit, B., Chattopadhyay, P., Sarkar, C., Gupta, D.K., Sinha, S. & Chosdol, K. (2018) FAT1 modulates EMT and stemness genes expression in hypoxic glioblastoma. *Int. J. Cancer*, **142**, 805-812.

Stevanovic, M., Kovacevic-Grujicic, N., Mojsin, M., Milivojevic, M. & Drakulic, D. (2021) SOX transcription factors and glioma stem cells: Choosing between stemness and differentiation. *World J. Stem Cells*, **13**, 1417-1445.

Wang, H., Tan, Y., Jia, H., Liu, D. & Liu, R. (2022) Posaconazole inhibits the stemness of cancer stem-like cells by inducing autophagy and suppressing the Wnt/beta-catenin/survivin signaling pathway in glioblastoma. *Front. Pharmacol.*, **13**, 905082.

Wang, R., Zhang, X., Huang, J., Feng, K., Zhang, Y., Wu, J., Ma, L., Zhu, A. & Di, L. (2023) Bio-fabricated nanodrugs with chemo-immunotherapy to inhibit glioma proliferation and recurrence. *J. Control. Release*, **354**, 572-587.

Wen, P.Y., Weller, M., Lee, E.Q., Alexander, B.M., Barnholtz-Sloan, J.S., Barthel, F.P., Batchelor, T.T., Bindra, R.S., Chang, S.M., Chiocca, E.A., Cloughesy, T.F., DeGroot, J.F., Galanis, E., Gilbert, M.R., Hegi, M.E., et al. (2020) Glioblastoma in adults: a Society for Neuro-Oncology (SNO) and European Society of Neuro-Oncology (EANO) consensus review on current management and future directions. *Neuro Oncol.*, **22**, 1073-1113.

Wen, Z., Chen, M., Guo, W., Guo, K., Du, P., Fang, Y., Gao, M. & Wang, Q. (2021) RORbeta suppresses the stemness of gastric cancer cells by downregulating the activity of the Wnt signaling pathway. *Oncol. Rep.*, **46**, 180.

Wen, Z., Pan, T., Yang, S., Liu, J., Tao, H., Zhao, Y., Xu, D., Shao, W., Wu, J., Liu, X., Wang, Y., Mao, J. & Zhu, Y. (2017) Up-regulated NRIP2 in colorectal cancer initiating cells modulates the Wnt pathway by targeting RORbeta. *Mol. Cancer*, **16**, 20.

Wu, J., Ji, Z., Liu, H., Liu, Y., Han, D., Shi, C., Shi, C., Wang, C., Yang, G., Chen, X., Shen, C., Li, H., Bi, Y., Zhang, D. & Zhao, S. (2013) Arsenic trioxide depletes cancer stem-like cells and inhibits repopulation of neurosphere derived from glioblastoma by downregulation of Notch pathway. *Toxicol. Lett.*, **220**, 61-69.

Zhao, J., Jiang, Y., Chen, L., Ma, Y., Zhang, H., Zhou, J., Li, H. & Jing, Z. (2021) The EIF4A3/CASC2/RORA Feedback Loop Regulates the Aggressive Phenotype in Glioblastomas. *Front. Oncol.*, **11**, 699933.

Zheng, L., Jiang, H., Zhang, Z.W., Wang, K.N., Wang, Q.F., Li, Q.L. & Jiang, T. (2016) Arsenic trioxide inhibits viability and induces apoptosis through reactivating the Wnt inhibitor secreted frizzled related protein-1 in prostate cancer cells. *Onco Targets Ther.*, **9**, 885-894.